

## **Visualizing Anderson Localization in 3d using Monte Carlo method**

S. Datta

Department of Theoretical Physics

Indian Association For the Cultivation of Science

2A & 2B Raja S. C. Mullick Road,

Kolkata 700 032, India

We study the effect of Anderson localization on a Bose-Einstein condensate in 3d in a disordered potential by Feynman-Kac path integral technique. Simulations are performed in continuous space using canonical ensemble. Owing to the high degree of control over the system parameters we also study the interplay of disorder and interaction in the system. We numerically compute the localization length, mobility edge and density profile of the condensate. We observe that as the interaction strength increases, the wave functions become more and more delocalized.

## 1 Introduction:

Anderson localization [1] (AL) corresponds to a quantum interference of the multiply scattered non-interacting particles from the random potentials and is characterized by the exponential decay of wave-function over a typical distance, the localization length. This kind of localization denies the possibility of ordinary conduction and diffusion and is not at all obvious. It was predicted fifty years ago in the context of the study of conductance of electrons in crystals. However, Anderson localization has not been observed for matter waves due to the complexity in the inherent structure of solids and the complex interaction associated with it. Fortunately the recent emergence of the field of ultracold physics offers new approaches for these issues due to the fact that the systems investigated are very clean, very dilute and very cold. In addition, the parameters involved in the interaction are so much controllable that ultracold atoms can realize quantum simulators i.e., they provide platforms to investigate various fundamental models which were hitherto inaccessible. In addition to this the interplay between the disorder and interaction is an important issue in condensed matter physics. The combination of ultracold atoms and the optical potential usually provides a platform to study disorder and interaction. A disordered potential can be realized either with laser speckles or quasi-periodic potentials and AL has been recently observed for both the disorder [2,3]. It is known that system in 1d and 2d the eigenstates are localized for all values of disorder strength. In 3d there exists an energy known as 'mobility edge' which separates the localized and extended states. Self consistent theory of localization enables one to calculate the localization length and mobility edge in 3d. But these are not fully exact. All of these issues call for investigations of AL in higher dimensions and thus the three dimensional localization is high on the agenda of several teams. Since Gross Pitaevski or other mean field techniques break down for strong interaction, we propose to study the effect of Anderson localization in cold atoms with Quantum Monte Carlo simulation based on Feynman-Kac path integration method. It is well known, a transition can be induced from the localized to the extended eigenstates ( Anderson delocalization ) in a disordered system by tuning the various parameters in the controllable interaction. Most of the theoretical calculations in Anderson localization have been done in 1d with mean field theory. Results from 1d systems do not always give the essence of a physical phenomenon correctly and are not directly comparable with experimental results. Mean field techniques yield good results as long as one is dealing with dilute gases with weak interactions but they fail to describe correctly the nature of different many body effects and provide a reliable estimate of various critical factors. The key ingredient which is missing in the mean field description is the proper account of interaction in the proposed model. That puts a challenge on the theoretical front to look for its non-perturbative and fully quantum mechanical counterpart and thereby motivates us we carry out a qualitative study of the many body effects using diffusion Monte Carlo method which has been proven very accurate in the strong interaction regime. Most of the work has been accomplished using lattice model and a very little has been done in the continuous phase space. This work would provide a method of computing localization lengths, mobility edges etc. beyond mean field regime in higher dimensions both at zero and finite temperature. In Section 1 we have included the introduction. In Section 2 we have described the model used in the simulation work and defined the different observables which are related to the many-body solution. Section 3 contains all the visualization plots related to 1d and 3d AL. Section 4 provides the numerical details of simulation technique and the precision of the numerical work. In section 5, we discuss the results of the various simulations.

## 2 The model:

### 2.1 Theory

We study the effect of Anderson localization of a system of  $100 \text{ Rb}^{87}$  atoms with a disordered potential and a short ranged interaction by Feynman-Kac path integral technique. Let us consider a Bose-Einstein condensate of 100 ( $N \gg 1$ ) atoms of mass  $m$  trapped in 3D spherically symmetric harmonic potential  $V_{\text{trap}}$ , a random potential  $V_R$  and a repulsive interaction  $V_{\text{int}}$ . In the Schrödinger picture the random Hamiltonian then can be represented as

$$H = -\frac{\Delta}{2} + V \quad \text{with} \quad V = V_{\text{trap}} + V_{\text{int}} + V_R$$

Mostly at  $T=0$ , Gross-Pitaevski (GP) technique is applied for the calculation of energy, density of a many body system. The mean field approach such as GP for solving many body dynamics is only approximate. We propose to apply Diffusion Monte Carlo technique known as Feynman-Kac path integral simulation to the above quantum gas. To connect Feynman-Kac (FK) or Generalized Feynman-Kac (GFK) to other many body techniques our numerical procedure has a straight-forward implementation[4,5] to Schrödinger's wave mechanics. For the Hamiltonian  $H = -\Delta/2 + V(x)$  consider the initial-value problem

$$\frac{dU(x,t)}{dt} = \left( \frac{\Delta}{2} - V(x) \right) \psi(x,t), \quad (1)$$

Where  $x \in \mathbb{R}^d$  with  $d = 3N$  and  $U(x,0)=1$ . The Feynman-Kac solution to this equation is

$$\psi(x,t) = E \exp \left[ - \int_0^t V(x(s)) ds \right], \quad (2)$$

Where  $x(t)$  is a Brownian motion trajectory and  $E$  is the average value of the exponential term with respect to these trajectories. The lowest energy eigenvalue for a given symmetry can be obtained from the large deviation principle of Donsker and Varadhan[6]

$$\lambda = - \lim_{t \rightarrow \infty} \frac{1}{t} \ln E \exp \left[ - \int_0^t V(x(s)) ds \right], \quad (3)$$

In dimension higher than 2, the trajectory  $x(t)$  escapes to infinity with probability 1. As a result, the important regions of the potential are sampled less and less frequently and the above equation converges slowly. Now for this analysis we do not incorporate importance sampling as the trial function chosen

would impose some localization in the system and this localization might overshadow the localization induced by the disorder. We merely employ the bare Feynman-Kac path integral technique here.

Now suppose  $V_R=0$  at  $t = t_0$ . Then following reference [7] the Schrödinger equation for the above Bose condensate reads as the following where  $\mu_c$  is the chemical potential of the Bose condensate. As soon as the  $V_R$  is turned on for  $t > t_0$  a new energy scale is created at the mobility edge  $\varepsilon_c$ .

$$[-\Delta/2 + V_{\text{int}} + V_{\text{trap}}]\psi_c(\vec{r}, t) = \mu_c \psi_c(\vec{r}, t)$$

$$\text{Where } V_{\text{trap}} = \frac{1}{2} \sum_i^N [x_i^2 + y_i^2 + z_i^2]$$

## 2.2 Observables and quantities of interest:

Numerical work with bare Feynman-Kac procedure employing modern computers was reported [8] for the first time for few electron systems after forty years of the original work [9] and seemed to be really useful for calculating atomic ground state [4]. A fairly good success in atomic physics motivated us to apply it Condensed matter Physics [5]. Here in this paper we apply Feynman-Kac procedure to Bose-Einstein Condensate of  $Rb^{87}$  to visualize Anderson localization in cold atoms. In this paper we calculate the many body density function, localization length, inverse participation number and imaginary time mean square displacement which are defined as follows.

**Many body Density:** The normalized version of the many body density in the coordinate representation can be represented by [10]

$$\rho(x_1, x_2, \dots, x_N; x'_1, x'_2, \dots, x'_N) = \sum_i w_i \psi_i(x_1 \dots x_N) \psi_i^*(x'_1 \dots x'_N)$$

$$\text{where } w_i = \frac{e^{-\beta E_i}}{\sum_i e^{-\beta E_i}}$$

$$\rho(x_1, x_2, \dots, x_N; x'_1, x'_2, \dots, x'_N; \beta) = \frac{\sum_i e^{-\beta E_i} \psi_i(x_1 \dots x_N) \psi_i^*(x'_1 \dots x'_N)}{\sum_i e^{-\beta E_i}}$$

For  $\beta \rightarrow \infty$ , only the ground state contributes or in other words

$$\sum_i e^{-\beta E_i} \psi_i(x_1 \dots x_N) \psi_i^*(x'_1 \dots x'_N) \rightarrow e^{-\beta E_0} \psi_0(x_1 \dots x_N) \psi_0^*(x'_1 \dots x'_N) \text{ and } \sum_i e^{-\beta E_i} \rightarrow e^{-\beta E_0}$$

Then the many body density becomes

$$\rho(x_1, x_2, \dots, x_N; x'_1, x'_2, \dots, x'_N; \beta) = \frac{e^{-\beta E_0} \psi_0(x_1 \dots x_N) \psi_0^*(x'_1 \dots x'_N)}{e^{-\beta E_0}}$$

$$\rho(x_1, x_2, \dots, x_N; x'_1, x'_2, \dots, x'_N) = \psi_0(x_1 \dots x_N) \psi_0^*(x'_1 \dots x'_N)$$

For diagonal density function becomes

$$\rho(x_1, x_2, \dots, x_N; x_1, x_2, \dots, x_N) = \psi_0^2(x_1, x_2, \dots, x_N)$$

In terms of Feynman-Kac solution the many body density matrix becomes

$$\rho(x_1, x_2, \dots, x_N; x_1, x_2, \dots, x_N) = |\psi(x, t)|^2 = \left| E \exp\left[-\int_0^t V(x(s)) ds\right] \right|^2$$

**Imaginary time mean square displacement:** An elegant way to distinguish between extended and localized states can be found by looking at their time evolution[11]. More precisely one can calculate the mean square distance  $r^2(t)$  travelled by the particle up to time  $t$  :

$$r^2(t) = \sum |x|^2 |\exp[itH]\Psi_0(x)|^2$$

$$= \sum |x|^2 |\Psi_t(x)|^2$$

where  $\Psi_0$  is the initial wave packet and  $\exp[itH]$  is the evolution operator. In the case of perfect periodic crystal or without any disorder in the system  $r^2(t)$  increases in time  $t$ , while in the case of localization  $r^2(t)$  is bounded uniformly with time. We calculate this quantity for all the localized states to probe for localization.

**Mobility Edge and Inverse Participation Number:** In order to decide whether or not a state is localized it is often sufficient to consider the second moment  $P = \sum_r |\Psi(r)|^4$ , Where  $\Psi(r)$  is the eigenvector of the corresponding symmetry state with eigenvalue  $E$ . The above quantity is called the inverse participation number (ipn) and it is nonzero if it falls on the interval of energy comprising localized states (pure point spectrum)[12] and vanishes for extended states (absolutely continuous spectrum).

### 3 Visualization of Anderson localization in 1d and 3d:

According to scaling theory of localization there is always localization in 1d. Apparently there is no point addressing the issue of Anderson localization in 1d. However we first study the localization in 1d as most of the 1d problems are solvable analytically and thus we can compare our numerical solutions to analytic solutions and standardize our codes. The interference effects which on a short length scale are responsible for the fluctuations in the amplitude of the eigenfunction and resulting reduction of the conductivity. As a matter of fact the eigenfunction exponentially decays to zero at a very large distance. The localization problem in 1d systems has been studied using various methods [13-19]. Exact analytical results and very accurate numerical data are available concerning the energy and disorder dependence of the localization length and probability distribution of various quantities of interest in 1d. Our interest is to study all these in 3d.

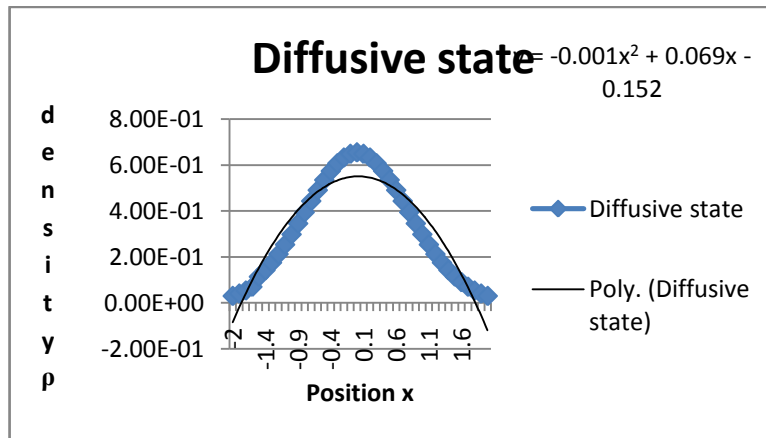


Fig 1 Ground state density of non interacting BEC in a trap potential in 1d

### 3.1 Localization in 1d with bi-chromatic potential:

We consider the motion of particles ( $(Rb^{87})$  atoms) in the following bi-chromatic potential (ref to Fig 2)

Underneath we use the parameters from the reference [20]

$$V_b = s_1 E_{R_1} \sin^2(k_1 x) + s_2 E_{R_2} \sin^2(k_2 x)$$

$$k_i = 2\pi/\lambda_i \quad E_{R_i} = \frac{\hbar^2}{2m\lambda_i^2}$$

$$s_1 = 10 \text{ and } s_2 = 2 \quad \lambda_1 = 830.7 \text{ nm} \quad \lambda_2 = 1076.8 \text{ nm}$$

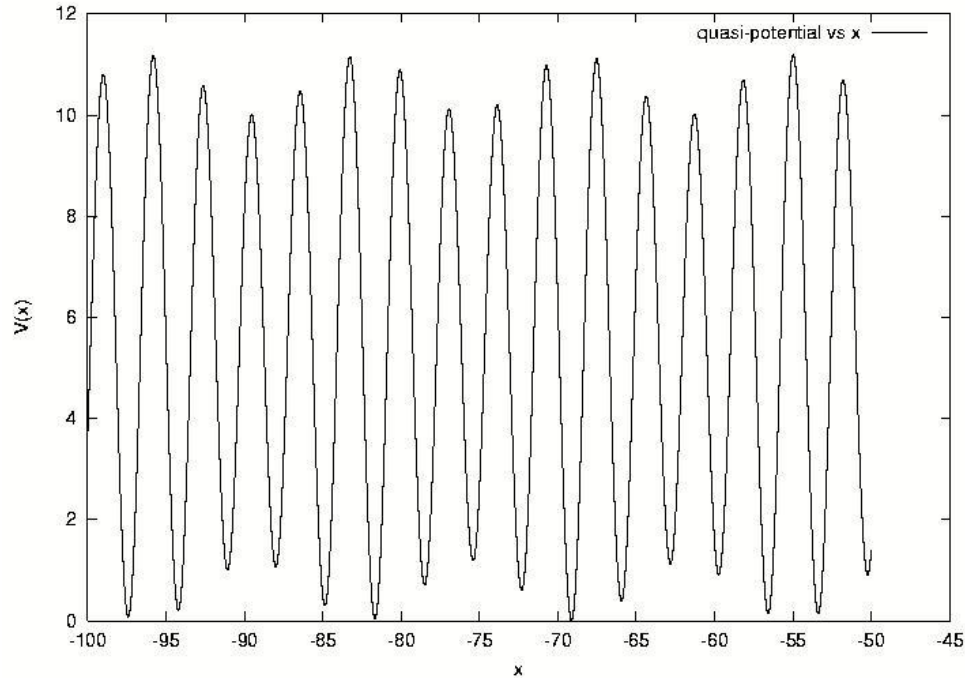


Fig 2 Plot of bi-chromatic potential  $s_1 = 10$  and  $s_2 = 2$   $\lambda_1 = 830.7 \text{ nm}$   $\lambda_2 = 1076.8 \text{ nm}$

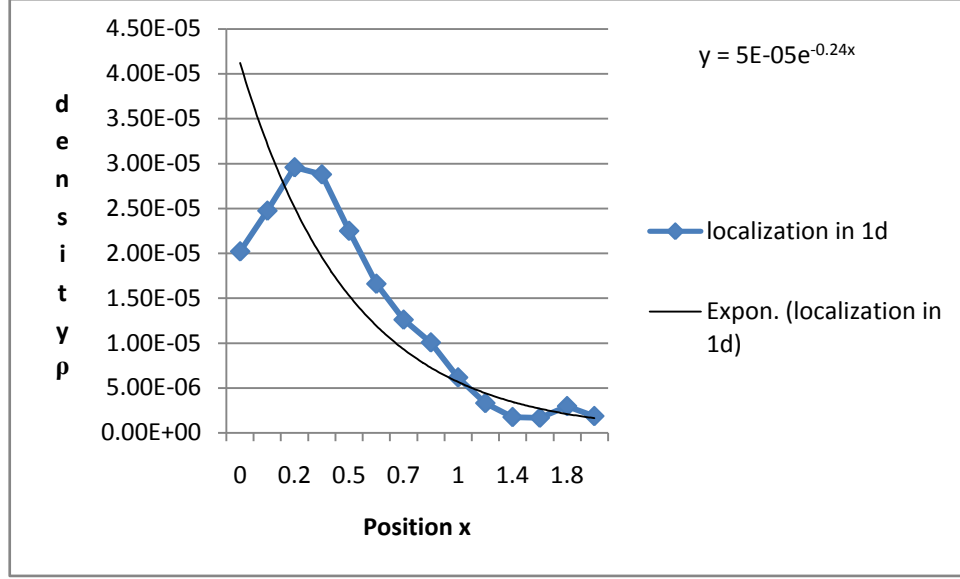


Fig 3. Anderson localization in 1d with quasi periodic potential

From exponential fit it turns out that the localization length is 4

### 3.2 Localization 3d BEC with one dimensional random potential.:

Next we consider the effect of random potential in  $Rb^{87}$  BEC in 3d. Previously the localization of

$$H = -\frac{\Delta}{2} + V_0 \delta(x - x_j) + V_{\text{trap}}$$

$$V_{\text{trap}} = \frac{1}{2} \sum_i^N [x_i^2 + y_i^2 + z_i^2]$$

In 1d one can adopt  $V_R(x) = V_\delta(x)$  and in 3d,  $V_R(\vec{r}) = V_\delta(\vec{r})$ . These are zero range interactions and these limits can be obtained from a finite range potential where the range approaches zero and strength is approximately adjusted. For the finite-range interaction we use a Gaussian interaction

$$V_G(\vec{r}) = V_0 e^{-r^2/2b^2}$$

Or in other words in performing the actual simulation we use Gaussian interaction as [21]

$$\lim_{b \rightarrow 0} V_G(\vec{r}) = V_\delta(\vec{r})$$

Underneath we have generated two plots (Fig 4(a) and Fig 4(b)) using data produced by the above form of delta function

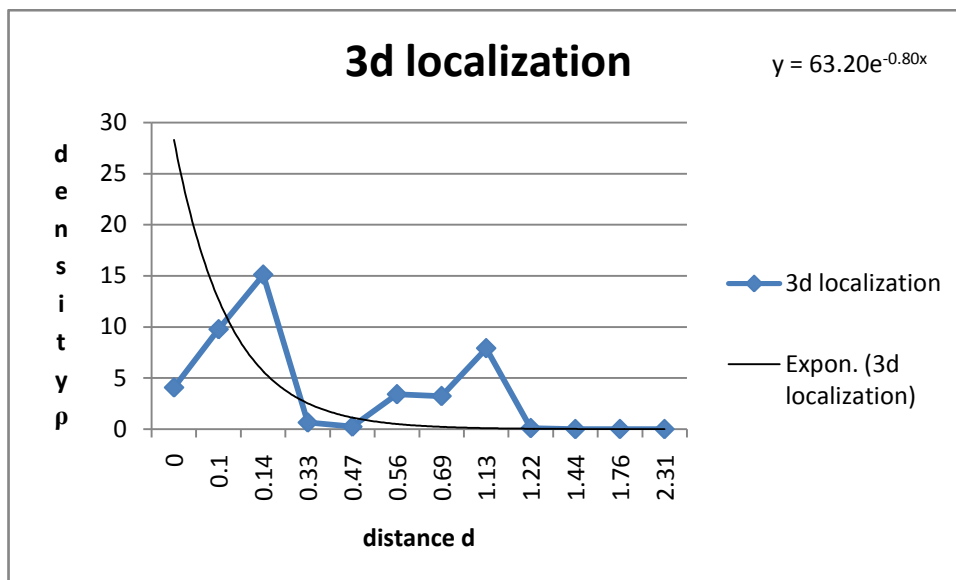


Fig 4(a) localization in 3d with random potential; plot of density vs distance 'd'

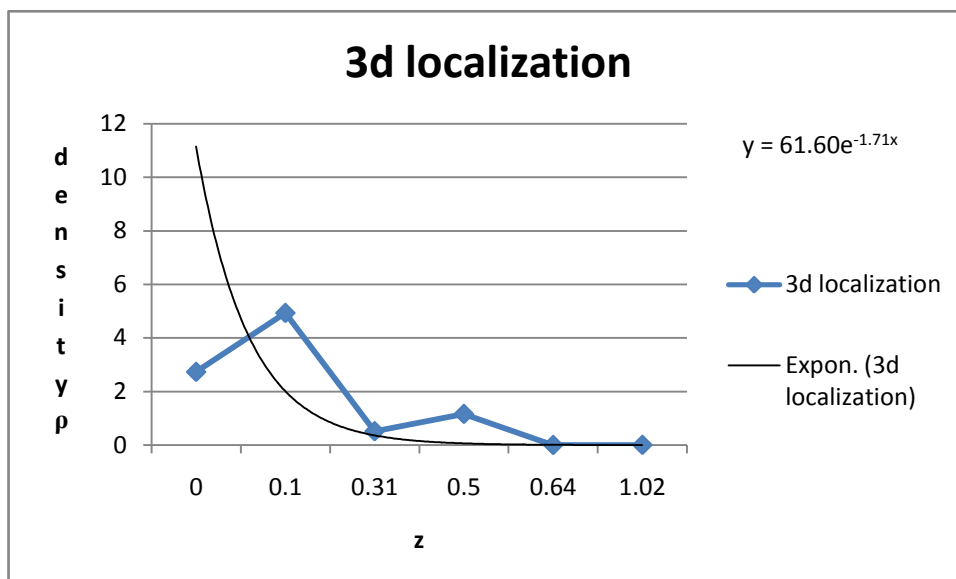


Fig 4(b) localization in 3d with random potential; plot of density vs  $z$



### 3.3 Calculation of the mobility edge:

From the definition of the mobility edge given in the Section 2.2 we plot Inverse Participation Number (ipn) with energy and observe that the critical energy after which the spectrum is continuous is 0.0729. This critical energy is the mobility edge for  $Rb^{87}$ .

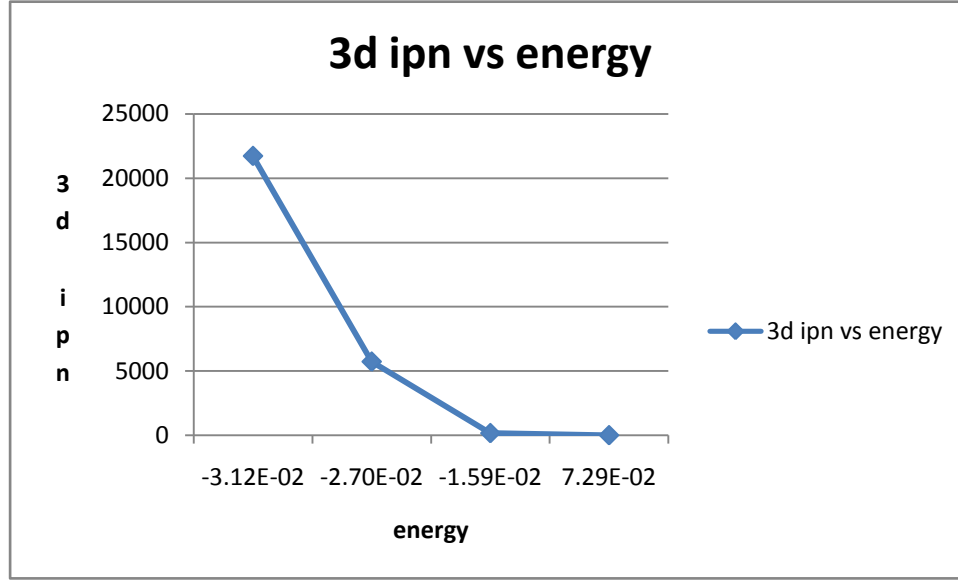


Fig 5 ipn vs energy in 3d

### 3.4 Delocalization in presence of interaction in the case of quasi-periodic potential.

Fig 6(a) shows the ground state of BEC. Fig 6(c)-Fig 6(e) show the effect of Morse interaction on the bi-chromatic potential. As the interaction strength 'g' increases the density profile becomes more and more coherent. As a result of introducing quasi-periodic disorder the periodicity of is partly broken as shown in the Fig 6(b) and the spectrum consists of both extended and localized states. By adding Morse interaction in the Hamiltonian the spectrum becomes more and more coherent (Fig 6(c)-Fig 6(d)). As a matter of fact the periodicity of Fig 6(a) is again restored in Fig 6(c) once a small amount of interaction g was incorporated in the quasi-random Hamiltonian. In Fig 6(e) we see that the effect of disorder is completely delocalized by the Morse interaction and we see a transition from Anderson glass to the coherent BEC again. Similar analysis has been done in ref [22]

$$[-\Delta/2 + V_{\text{int}} + V_{\text{trap}} + V_b]\psi_c(\vec{r}, t) = \mu_c \psi_c(\vec{r}, t)$$

$$\text{Where } V_{\text{trap}} = \frac{1}{2} \sum_i^N [x_i^2 + y_i^2 + z_i^2]$$

$$V_{\text{int}} = V_{\text{Morse}} = \sum_{i,j} V(r_{ij}) = \sum_{i < j} g[e^{-\alpha(r-r_0)}(e^{-\alpha(r-r_0)} - 2)]$$

$$V_b = s_1 E_{R_1} \sin^2(k_1 x) + s_2 E_{R_2} \sin^2(k_2 x)$$

$$k_i = 2\pi/\lambda_i \quad E_{R_i} = \frac{h^2}{2\pi\lambda_i^2}$$

$$s_1 = 10 \text{ and } s_2 = 2 \quad \lambda_1 = 830.7 \text{ nm} \quad \lambda_2 = 1076.8 \text{ nm}$$

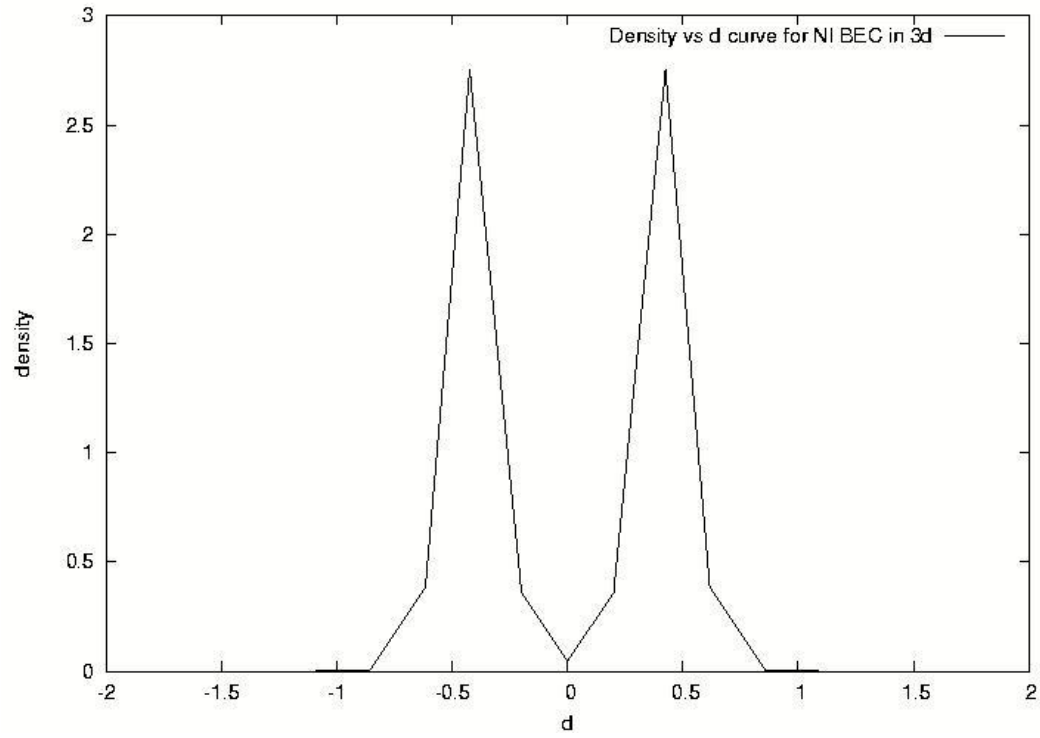


Fig 6(a) Density vs d curve for non-interacting BEC in 3d

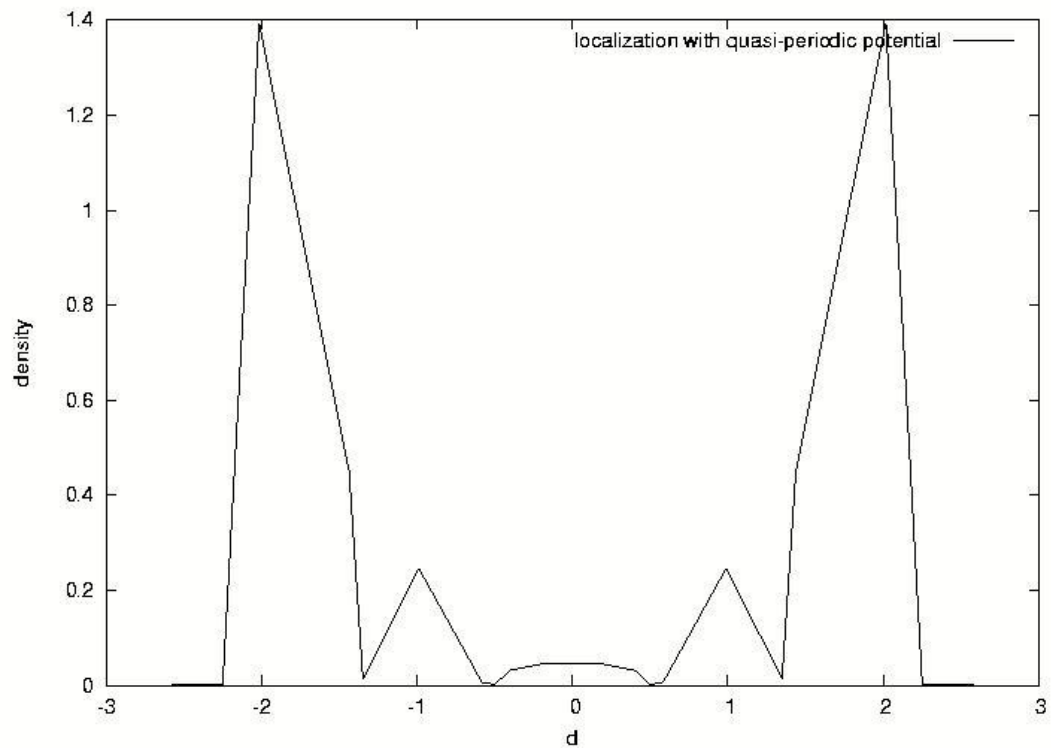


Fig 6(b) localized and extended states in 3d with quasi potential

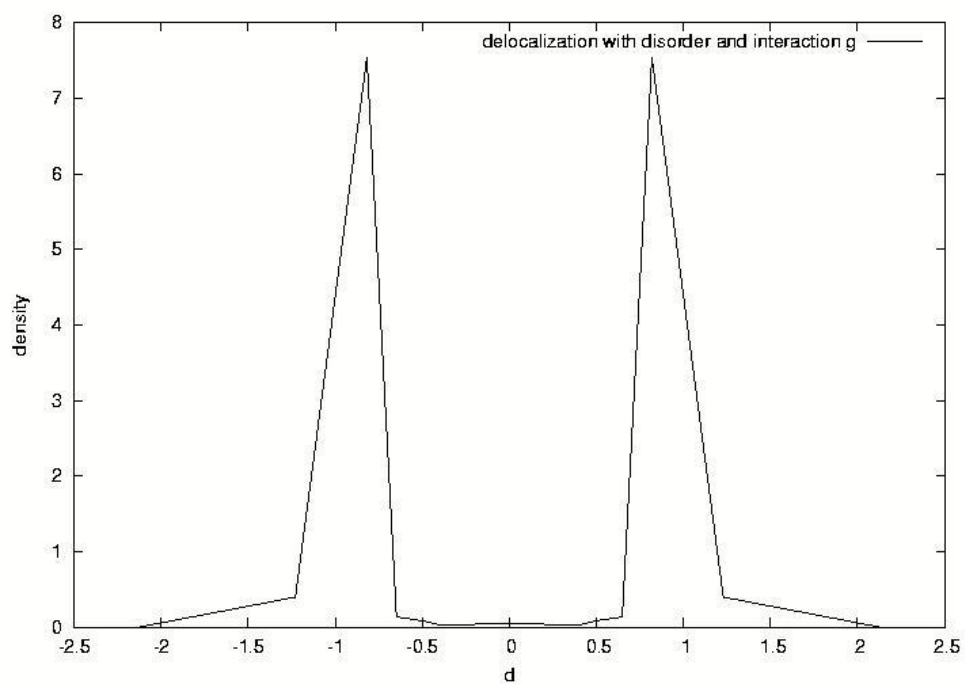


Fig 6(c) delocalization in 3d with disorder and interaction  $g$

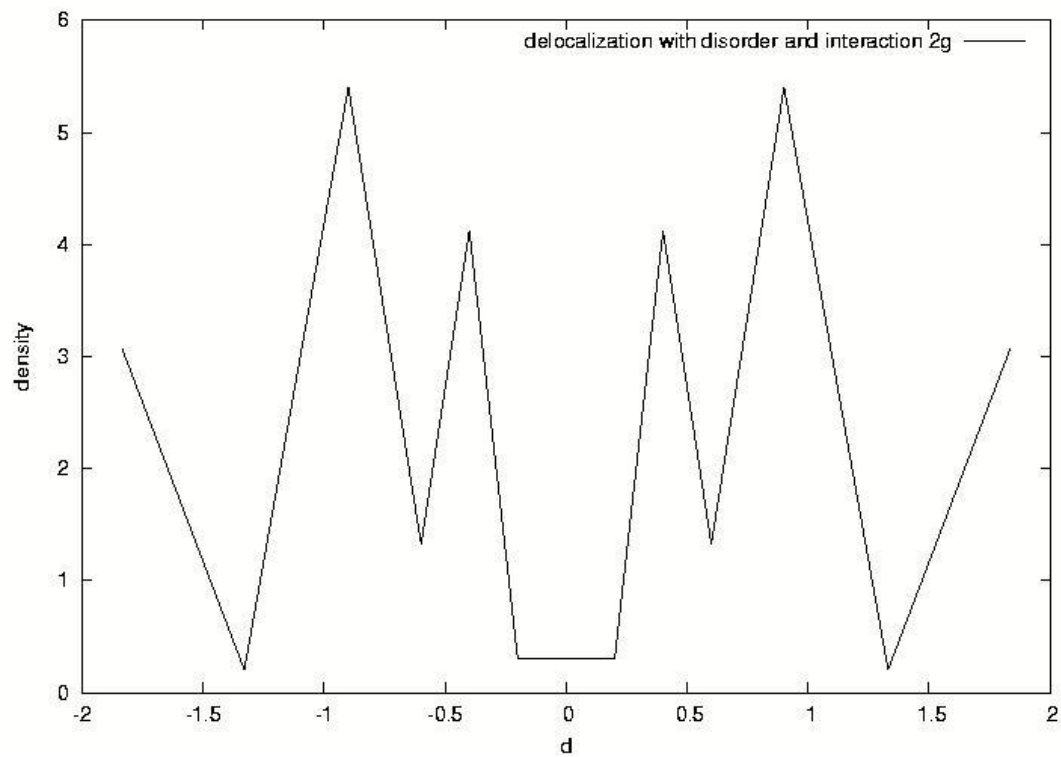


Fig 6(d) delocalization in 3d with disorder and interaction 2g

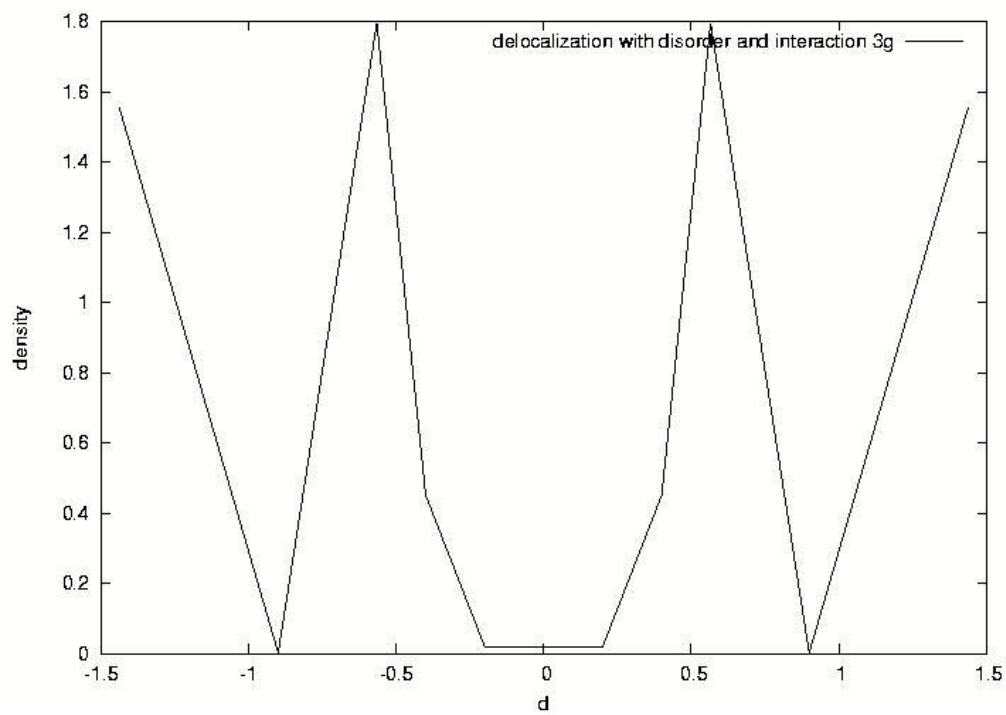


Fig 6(e) complete delocalization in 3d with disorder and interaction 3g

### 3.5 Delocalization in presence of interaction in the case of speckle potential.

We also consider the motion of particles (  $87_{Rb}$  atoms ) in the speckle potential. To visualize the speckle potential we adopt the same analytic form of repulsive sech-squared-shape potential as used in the ref [23-24]: In fig 7(a) we observe the localization effect due to the above speckle potential and in Fig 7(b) and Fig 7(c) we see the effect of delocalization due to the Morse potential .

$$V(z) = b * \text{sech}^2\left(\frac{z}{\beta}\right).$$

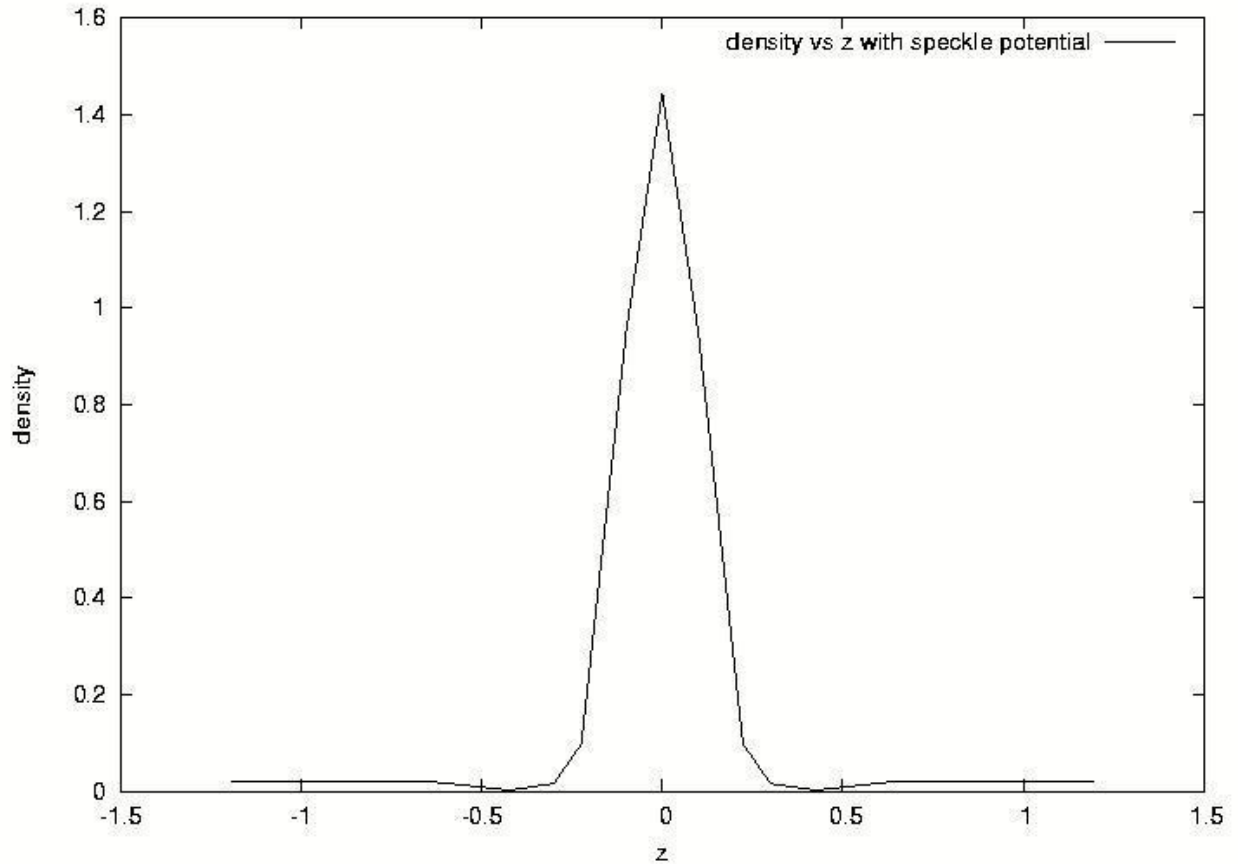


Fig 7(a) Localization in presence of speckle potential

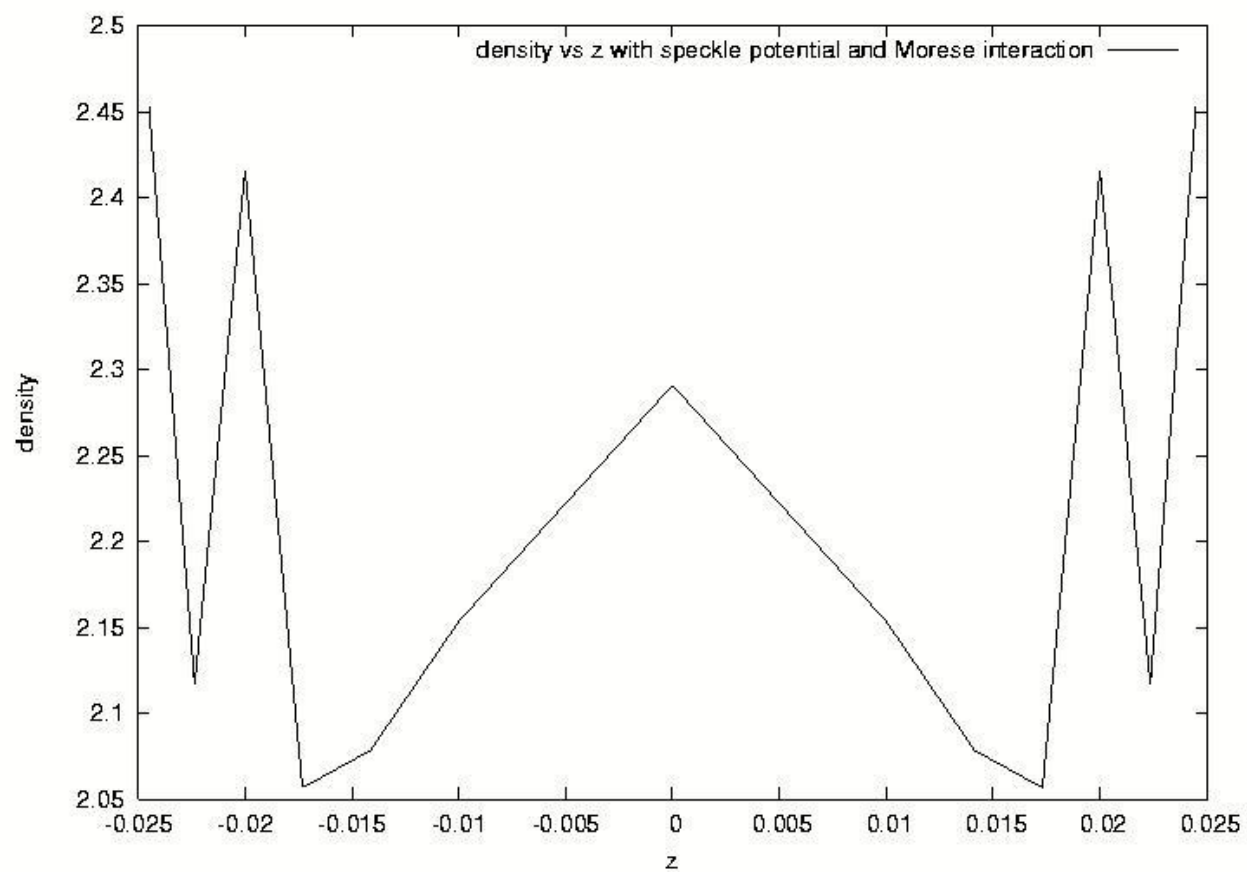


Fig 7(b) delocalization with speckle potential and Morse interaction

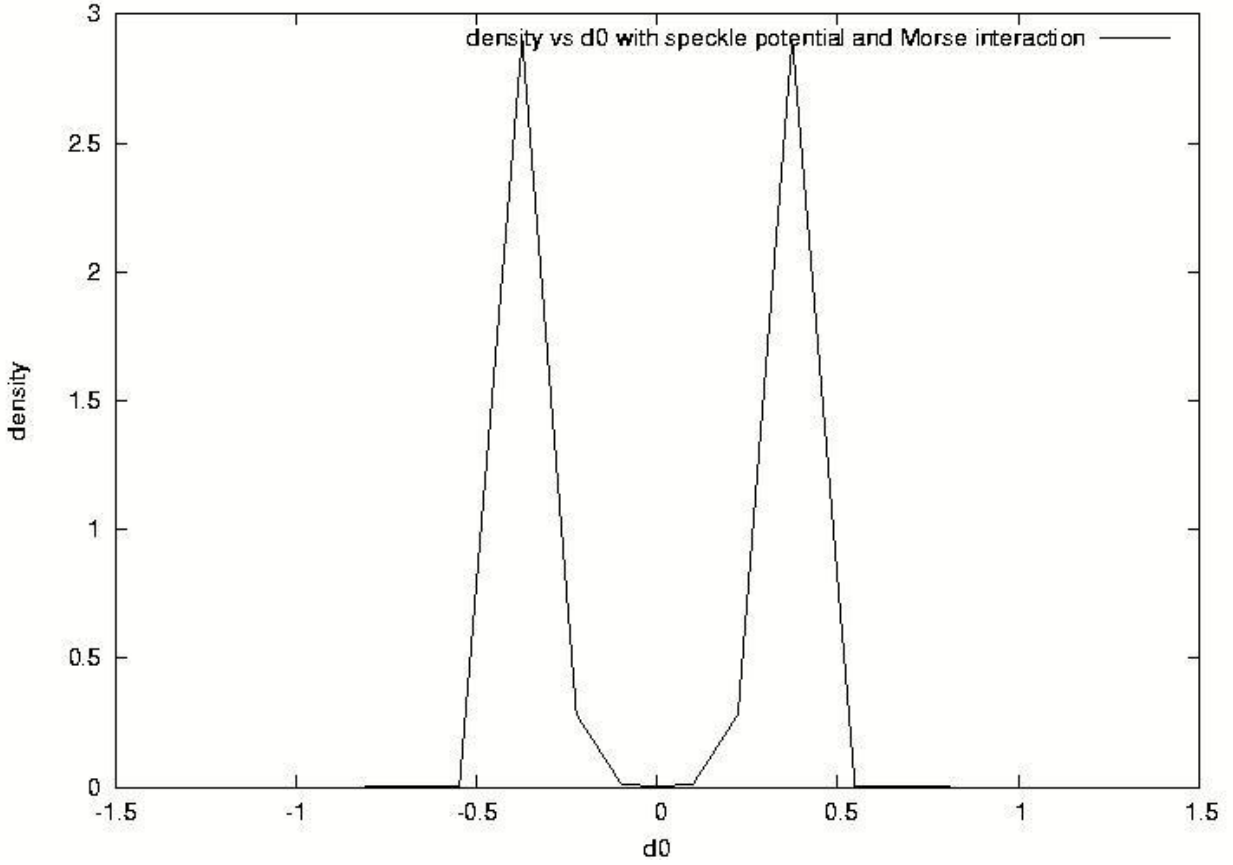


Fig 7(c) Complete delocalization

#### 4 Numerical details and the precision of the calculations.

##### 4.1 Numerical details:

The formalism given in the Section 2 is valid for any arbitrary dimensions  $d$  (for a system of  $N$  particles in three dimensions  $d = 3N$ ). Generalizations of the class of potential functions for which Eqns 2 and 3 are valid are given by Simon [25] and include most physically interesting potentials, positive or negative, including, in particular, potentials with  $1/x$  singularities. It can be argued that the functions determined by Eq(3) will be the one with the lowest energy of all possible functions independent of symmetry. Although other interpretations are interesting, the simplest is that the Brownian motion distribution is just a useful mathematical construction which allows one to extract the other physically relevant quantities like density, mean square displacement along with the ground and the excited state energy of a quantum mechanical system. In numerical implementation of the Eq(2) the  $3N$  dimensional Brownian motion is replaced by  $3N$  independent, properly scaled one dimensional random walks as follows. For a given time  $t$  and integer  $n$  and  $l$  define [26] the vector in  $R^{3N}$ .

$$W(l) \equiv W(t, n, l) = (w_1^1(t, n, l), w_2^1(t, n, l), w_3^1(t, n, l), \dots, w_1^N(t, n, l), w_2^N(t, n, l), w_3^N(t, n, l))$$

$$\text{where } w_j^i(t, n, l) = \sum_{k=1}^l \frac{\epsilon_{jk}^i}{\sqrt{n}}$$

with  $w_j^i(t, n, l) = 0$  for  $i = 1, 2, \dots, N; j = 1, 2, 3$  and  $l = 1, 2, \dots, nt$ . Here  $\epsilon$  is chosen independently and randomly with probability  $P$  for all  $i, j, k$  such that  $P(\epsilon_{jk}^i = 1) = P(\epsilon_{jk}^i = -1) = \frac{1}{2}$ . It is known by an invariance principle [27] that for every  $\nu$  and  $W(l)$  defined above .

$$\lim_{n \rightarrow \infty} P\left(\frac{1}{n} \sum_{l=1}^{nt} V(W(l))\right) \leq \nu$$

$$= P\left(\int_0^t V(X(s)) ds \leq \nu\right)$$

Consequently for large  $n$ ,

$$P\left[\exp\left(-\frac{1}{n} \int_0^t V(X(s)) ds\right) \leq \nu\right]$$

$$\approx P\left[\exp\left(-\frac{1}{n} \sum_{l=1}^{nt} V(W(l))\right) \leq \nu\right]$$

By generating  $N_{rep}$  independent replications  $Z_1, Z_2, \dots, Z_{N_{rep}}$  of

$$Z_m = \exp\left(-\frac{1}{n} \sum_{l=1}^{nt} V(W(l))\right)$$

And using the law of large numbers,  $(Z_1 + Z_2 + \dots + Z_{N_{rep}}) / N_{rep} = Z(t)$  is an approximation to Eq(2)

Here  $W^m(l), m = 1, 2, \dots, N_{rep}$  denotes the  $m^{th}$  realization of  $W(l)$  out of  $N_{rep}$  independently run simulations. In the limit of large  $t$  and  $N_{rep}$  this approximation approaches an equality and forms the basis of a computational scheme for the solution of a many particle system with a prescribed symmetry.

#### 4.2 Precision of the data associated with the calculations of Ground state density of non-interacting BEC in 1d with number of paths( $N_{rep}$ ) = 100000, $n=900$ and $t=1$ relevant to Fig (1)

x	Exact solution	FK solution	Exact density	FK density (this work)	error
0	0.80501	0.80508	0.64804	0.64815	-0.00011
.1	0.80195	0.80167	0.64312	0.64268	0.00044
.6	0.70189	0.70019	0.49264	0.49027	0.00237
1.1	0.50780	0.50566	0.25786	0.25569	0.00217
1.6	0.30369	0.30200	0.09220	0.09120	0.001

For more details in numerical analysis, one should take a look at one of our previous papers [28]



#### 4.2 Variation of Imaginary Time Mean square displacement with time $t$ for BEC in 1d without the random potential with number of paths $N_{rep} = 1$ , $n=900$ and $t=8-48$ with reference to Fig 1

Imaginary Time Mean square displacement  $r^2(t) = \sum |x|^2 |\exp[itH]\phi_0(x)|^2$

t	Random potential	mean square distance
8	0	62561.594101
16	0	191812.368405
24	0	438610.445992
32	0	1230319.373950
40	0	2323076.110784
48	0	3697358.142701

We observe that without the random potential the Imaginary Time Mean square displacement increases with time. We also find that if the random potential is included in the form of a 1d Gaussian potential the mean square distance is bounded by  $1.02509 \times 10^{-3}$ .

**5 Discussions:** From our observation we find that always in 1d and sometimes in 3d the wave functions in random potentials are localized. The incommensurate case is intermediate and is sometimes localized and sometimes extended. This establishes the fact there exists, a mobility edge which separates the point and extended spectrum. We visualize that as bi-chromatic potential can induce localization in a system of cold atoms, it is worth using this potential as an effective tool for implementing quasi-disorder in the case of an actual experiment. We also observe that interaction delocalizes the effect of disorder in Bose system in 3d. We verify in for each localized state the mean square distance is bounded and for the diffusive state the mean square distance grows with time. The other work in 3d which are worth mentioning can be found in the literature [29-31]. In the future we would like to study the density of states and critical exponents for these systems. Currently we are also trying to simulate the recent experiment [32] on the non-interacting gas of  $K^{40}$  to observe the three-dimensional Anderson Localization of spin polarized ultracold matter.

**Acknowledgements:** This work was partially supported by the Department of Science and Technology, India (award no SR/WOS A/PS-32/2009)

## References:

- [1]. P. W. Anderson, Phys. Rev. **109**, 1958
- [2]. Billy et al Nature 453 891 2008
- [3]. G Roati Nature **453** 895-898 2008
- [4]. Sumita Datta et al Phys. Rev A 61 030502(R) 2000, S Datta Ph D dissertation, The University of Texas at Arlington, USA
- [5]. S Datta, ( Cond-mat/0511647 ) Int. J of Mod Phys B, **22**, 4261-4273, 2008.
- [6] M D Donsker and M Kac J. Res. Natl. Bur. Stand. 44 581 1950
- [7] S. E. Skipetrov et al Phys. Rev Lett **100**,165301, 2008
- [8] A Korzeniewski, J L. Fry, D. E Orr and N. G. Fazleev, Phys. Rev Lett.**69**, 893 1992
- [9] M. D. Donsker and M Kac, J Res Natl. Bur. Stand, 44,581,1950,see also, M Kac in Proceedings of the Second Berkley Symposium( Berkley Press, California, 1951)
- [10] R. P. Feynman, Statistical Mechanics (Addison-Wesley Publishing Company,1972
- [11] F Martinelli and E.Scoppola Rev Del Nuovo Cimento **10**,1,1987
- [12](a) X Deng, Eur Phys J B **68** 435-443 2009  
(b) Biroli et al Progress in Theoretical Physics supplement no **184**, 187,2010
- [13] M Larcher, F Dalfovo and M. Modugno Phys Rev A **80**,053606, 2009
- [14] E Lucioni et al Phys Rev Lett **106**, 230403,2011
- [15] T Paul et al Phys Rev A 80,033615 (2009)
- [16] M Larcher, M. Modugno and F Dalfovo, phys rev A 83,013624, 2011
- [17] M Moratti and M Modugno arXiv:1102.5299v1 [cond-mat.quant-gas]
- [18] L Sanchez-Palencia et al New J Phys. **10** 045019 2008
- [19]. P Lugan et al Phys Rev A **80** 023605 2009
- [20] J.E. Lye et al Phys rev a **75**, 061603(R),2007
- [21] O Sorensen,D V Fedorov and A. S. Jensen J Phys B **37** 93-116 2004
- [22] Deissler et al Nature Physics **6**,354, 2010
- [23] M Modugno, Phys Rev A **73**, 013606, 2006

- [24] C Lee and J Brand, arXiv:cond-mat/0505697v37 Dec 2005
- [25] B Simon, Functional Integrals and Quantum Mechanics ( Academic Press, New York,1979)
- [26]A Korzeniowski, J Comp and App Math,**66**,333,1996
- [27] P. B. Billingsley, Convergence of Probability Measures (Wiley, New York,1968)
- [28]J. M. Rejcek, S Datta , N. G. Fazleev, J. L. Fry and A Korzeniowski, Computer Physics Communications, **105**,108-126, 1997.
- [29] P. Massigan et al arXivcond-mat/0604232 v2,2006
- [30] C. Conti and A. Fratalocchi, Nature Physics 4, 794, 2008
- [31]C. M. Soukoulis, A. D. Zdetsis and E. N. Economou, Phys Rev B **34**, 2253,1986
- [32] S. S. Kondov et al Science **334**,66,2011